A flexibility product for electric water heater aggregators on electricity markets

A flexibility product for electric water heater aggregators on electricity markets

Marie Pied
Polytechnique Montréal & GERAD
Email: marie.pied@polymtl.ca

Miguel F. Anjos
University of Edinburgh & GERAD
anjos@stanfordalumni.org

Roland P. Malhamé
Polytechnique Montréal & GERAD
Email: roland.malhame@polymtl.ca

May 5, 2020

Abstract: Electric thermal loads, such as those for space heaters, water heaters and air conditioners, due to their association with energy storage, are deferrable. Thus, they can become an effective tool to compensate for the mismatches between power generation and power demand induced by renewable sources. Load reduction and load increase may appear to be equivalent to generation increase and generation withdrawal, but there is a significant difference in the associated post-load-control energy rebound phenomena. These phenomena can provoke undesirable post-load-control changes in the demand dynamics. The contribution of this paper is twofold. First, we define a flexibility product that load aggregators could propose that would involve a mean energy increase or decrease offer for a price and also guarantee bounds on the post-load-control deviations from normal. Second, we provide aggregators with the mathematical tools to specify the maximum load relief or increase possible under specific constraints on post-control recovery dynamics. The analysis rests on successive solutions of a linear program and exploits recent results on load control based on mean field game theory. We consider the case of aggregate electric water heater loads.

Keywords: Energy market; mean field game theory; load control; demand response; aggregator; rebound

1 Introduction

Many jurisdictions have adopted energy transition policies that focus on increasing the use of intermittent renewable energy sources in the electricity mix [7]. However, the introduction of such sources brings new challenges linked to the instability they can potentially bring to the electricity grid because their power generation is highly variable. To increase the integration of power produced by these sources, it is essential to ensure a balance between generation and demand. This balance is often achieved by generation with a high marginal cost such as the use of gas-fired plants (when renewable power is insufficient) or reductions in renewable energy (when too much is available). Load management is thus a promising way to support the greater integration of renewables.

Load management or demand response (DR) consists in controlling flexible loads to compensate for fluctuation in generation. Much research has focused on quantifying the DR potential for peak reduction and load shifting, e.g., by reducing the peak on hot days [20] or by energy sharing among prosumers [3]. Projects such as PowerShift Atlantic [28] have demonstrated that this is both

technically possible and economically promising. In many places worldwide, including Ontario (Canada), industrial customers can already participate in DR programs [11].

To make residential load management programs possible and to integrate this flexibility into energy markets, a new entity is needed: the aggregator. Indeed, on its own, a residential building has only a negligible impact on the generation/load balance of the grid, but a group of such loads can have a significant impact. The role of the aggregator is thus to offer a flexibility product on the electricity market while incentivizing consumer participation. (For a discussion of the need for more aggregators in Europe, see [6]; for a hierarchical model with competing aggregators, see [5]). In particular, residential customers can participate via the energy storage potential of devices such as batteries, electric water heaters (EWHs), electric space-heaters and air conditioners. However, introducing this new player into the market requires new regulations and policies, as argued in [18] and [30], so that aggregators can really develop. Few studies address the important question of the nature of the offers that aggregators of residential loads can reasonably make [23].

Moreover, there are major barriers to entry for investors and customers, which limit the benefits of storage on the grid. These barriers are discussed in [27], and [8] makes a strong case for their removal in the context of California. [2] discusses the barriers in the European context and proposes a new regulatory framework. The main challenge is the fact that the current market structure in many regions does not accurately compensate flexible resources for the benefits they provide [9]. This motivates our design of a novel flexibility product that could be offered on the energy markets to maximize the value of residential energy storage.

There are various studies of flexibility products from the point of view of the aggregator. Some assess the potential flexibility without determining the specific load control needed to achieve such flexibility. For example, [26] focuses on the macroscopic/aggregator level and uses a mixed integer linear programming approach with two phases to provide a DR program optimizing the cost and benefits for aggregators and end-users. Similarly, [1] considers small commercial and residential buildings to study the potential flexibility taking into account the comfort of the occupants (from the point of view of the aggregator) without specifying how dispatchable loads are controlled to achieve the flexibility target.

Other studies focus on specific load types and study the controls needed to achieve the desired flexibility. Our paper is in this category: we study the EWH control that provides flexibility when aggregated. Other approaches in this category include [4], which uses a robust optimization to address the management of thermal loads, such as EWHs, and battery storage with the integration of photovoltaic electric sources. The authors consider the question of uncertainties and incorporate battery degradation, using 25 Portuguese households as a testbed. The aggregation of small prosumers in the Iberian market is studied in [13]: the authors develop a two-stage stochastic optimization model to support the aggregator. The approach in [35] optimizes the benefits of the group of consumers with a focus on the real-time energy market; it models thermal loads with typical centralized ON/OFF controls. Similarly, the work in [29] is concerned with the aggregation of residential consumers considering EWH and battery storage systems and seeks to maximize cost savings while ensuring a minimum level of comfort. The study is based on a market analysis and considers centralized ON/OFF controls.

One aspect in which our study differs from these is in the nature of the EWH control: we consider a decentralized and more complex control based on the theory of mean field games (MFGs). MFGs were introduced by [19] and developed independently in the engineering literature by [10]. Another aspect is that all these papers assume that the aggregator can affect the consumers' loads throughout the day. We make the more realistic assumption that the aggregator's control applies to specific time periods. Consequently, we define a flexibility product that can be purchased during a certain time interval; during that interval it can be viewed by the utility as a set of dispatchable

sources of load reductions or increases. Since the product is time-limited, we include constraints on what happens when the aggregator's control has ended, when it is desirable to avoid a rebound peak; see [24] for a discussion of rebound damping in a large heat-pump study.

We argue that because of the peculiarities of DR or equivalently demand dispatch (DD), including in particular systematic rebound or payback phenomena following the application of controls, a new class of DR-specific products must be defined. Our contribution is twofold. First, we define a novel load flexibility product that could be offered on the energy markets and which, beyond specifying a mean load reduction or increase over a fixed time period, provides guarantees on the size of post-load-control rebound dynamics, all relative to a normal base case consumption pattern. Second, assuming the adoption of a recently proposed collective load control methodology [16] based on the theory of MFGs, we develop an algorithm based on linear programming and simulation that an aggregator could use to assess the maximum offer it can propose within the constraints of the product.

MFG theory [10, 19] lies at the intersection of statistical mechanics, game theory and optimization. It is devoted to the analysis of games with many players who have a negligible individual impact but collectively create a stable mass effect. The corresponding controls have several advantages, including decentralization and communication parsimony. In this paper we build our analysis on the MFG-based load control strategy introduced in [16] and further discussed in [17], which is ideally suited for aggregator-based coordination of many deferrable loads. Closely related to the MFG methodology is a hierarchical load control strategy for the maximum integration of renewable sources explored in the SMARTdesc project at Polytechnique Montreal (see [21], [31] and [33]). It relies in particular on the deferrability of EWH loads, the same class of loads that we consider.

The hierarchical load-control methodology that we assume has two levels:
(i) *A macroscopic level* for the aggregator's planning decisions. At this level, the collection of controlled EWHs is represented as a *single-layer* massive water heater with a volume equal to the sum of the volumes of the individual controlled EWHs; a single heating element with a power rating equal to the sum of the power ratings of the individual EWHs; a deterministic hot-water energy extraction process corresponding to a scaled-up version of the mean individual hot-water energy extraction processes; and temperature constraints identical to those of the individual EWHs. Using this macro model the aggregator determines a realistic schedule of energy reductions or increases with rebound constraints that it can offer on energy markets.
(ii) *A microscopic individual EWH level* where the global targets set by the aggregator are collectively met via decentralized locally computed feedback-control policies based on MFG theory. The individual EWH models at this level are much more detailed and involve in general more than one uniformly mixed layer (two for the analysis reported in this paper).

The rest of the paper is structured as follows. In Section 2, we define our novel rebound-constrained aggregator-proposed load flexibility product. Sections 3, 4 and 5 provide the technical background for the assumed hierarchical load-control methodology. The microscopic individual stochastic EWH load model is described in Section 3. In Section 4, we review the elements of a prescriptive game framework whereby the aggregator sends an overall mean temperature target to the group of EWHs under its supervision, and each EWH responds with a locally computed and implemented control, consistent with its current ability to contribute to the global energy increase or decrease objective. The computation of the individual EWH control laws involves the approximate fixed-point mean temperature trajectory calculation detailed in Section 5. In Section 6, using the tools developed in the previous sections, we present a recursive algorithm based on linear programming and Monte Carlo simulation. It helps the aggregator to assess the maximum mean load increase or decrease it can offer, while satisfying a constraint on the size of the post-

load-control deviations from nominal uncontrolled behavior, as a result of a payback phenomenon. Section 7 presents a case study illustrating the calculations involved, together with a profitability analysis for the aggregator under different assumptions on the incentives it can offer. Section 8 summarizes our conclusions and discusses directions for further research.

2 Flexibility product definition

The flexibility product developed in this paper can be seen as the following function:

$$F(\bar{c}_W, T_{start}, T_{end}, t_{rebound}, r_{rebound})$$

where $\bar{c}_W$ represents the average load reduction or increase offered by the aggregator on the time interval T_{start} to T_{end}, relative to an agreed "nominal" load demand curve for the group of EWHs and for the time period of interest. During this period, the control implemented will be MFG-based. The sign of $\bar{c}_W$ is negative for a proposed load reduction or positive for an increase. Furthermore, the aggregator guarantees that on the interval $[T_{end}, T_{end} + t_{rebound}]$ the deviation of the collective EWH load from the nominal because of payback phenomena [34] will not exceed a percentage $r_{rebound}$.

3 Individual water heater model at the microscopic level

Nomenclature

Parameters

$\dot{m}_t^{in}$	Rate of water extraction at time t in kg/s
x_{env}	Temperature of the EWH surroundings in $°C$
x_{in}	Inlet water temperature in $°C$
M_l	water mass in layer l in kg
A_l	Lateral surface of layer l in m^2
C_{pf}	Specific heat of the fluid in $J/(kgK)$
U	Loss coefficient between tank and surroundings in $J/(m^2Ks)$
$\dot{V}^{mix}$	Water flow of extraction in l/s

Variables

$x_{l,t}$	Temperature of layer l at time t in $°C$
$\bar{u}_{l,t}$	Power from heating at layer l at time t in W

To describe the dynamics of the temperature of a EWH, we model the tank using $n = 2$ equal perfectly mixed volume layers, i.e., with uniform temperature as shown in Figure 1. Note that the figure includes one heating element per uniformly mixed water layer. In reality there is only one heating element, in the bottom layer, but we include separate (virtual) heating elements in other layers to compensate for modeling imperfections. We do not model the convection phenomena that allow heat to travel from the bottom layers toward the top layers in the absence of water draws; they would jeopardize the linearity of our model and thus complicate our MFG analysis. The heating rate of the actual EWH heating element can be calculated as the sum of the heating rates

of the fictitious heating elements computed on the basis of our linear model. This type of model reflects the stratification of temperature in a typical tank. We used just two layers to simplify the computations, but the analysis can be extended to n layers.

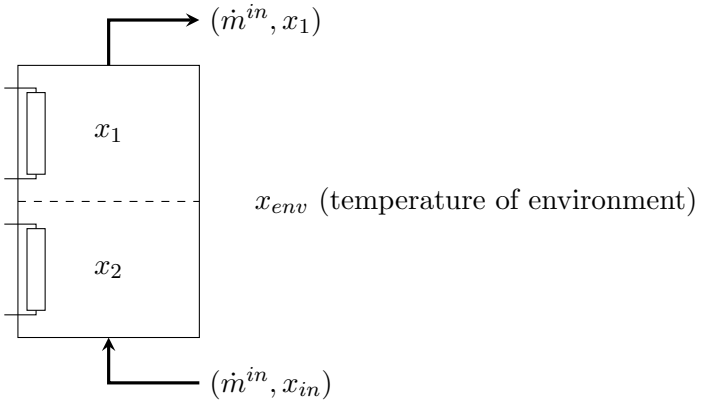

Figure 1: EWH model showing tank with two perfectly mixed layers; water is input and extracted at the same rate but at different temperatures.

The thermal dynamics are described by the energy balance in each layer:

$$M_1 C_{pf} \frac{dx_{1,t}}{dt} = UA_1(x_{env} - x_{1,t}) + \bar{u}_{1,t} + \dot{m}_t^{in} C_{pf}(x_{2,t} - x_{1,t}) \tag{1a}$$

$$M_2 C_{pf} \frac{dx_{2,t}}{dt} = UA_2(x_{env} - x_{2,t}) + \bar{u}_{2,t} + \dot{m}_t^{in} C_{pf}(x_{in,t} - x_{2,t}) \tag{1b}$$

Note that $\dot{m}_t^{in}$ is modeled as a piecewise constant hot-water extraction ON-OFF process. It has time-dependent extraction, and the transition rate evolves according to a continuous time Markov chain, with the states θ_t taking values in $\Theta = \{0, 1\}$. From state 0, the Markov chain switches to state 1 according to a exponential law with rate α_0, and from state 1 it switches to state 0 according to a exponential law with rate α_1. As discussed in [22], one can introduce an infinitesimal generator $L = \begin{pmatrix} -\alpha_0 & \alpha_0 \\ \alpha_1 & -\alpha_1 \end{pmatrix}$ and the probability $\zeta_{j,t}$ for the Markov chain θ_t to be in state $j \in \{0, 1\}$ at time t: $\zeta_t = [\zeta_{0,t}, \zeta_{1,t}]$ with $\frac{d\zeta_t}{dt} = \zeta_t L^T$.

State $j = 0$ represents the absence of extraction of water, and state $j = 1$ represents the presence of such extraction at time t with flow $\dot{V}^{mix}$ so we have $\dot{m}_t^{in} = \theta_t \dot{V}^{mix}$. Equations (1a) and (1b) can be written in matrix form as follows:

- $x_t = (x_{1,t}, x_{2,t})^T$
- $\bar{u}_t = (\bar{u}_{1,t}, \bar{u}_{2,t})^T$
- $A(\theta_t) = \begin{pmatrix} -\dfrac{A_1 U + \dot{m}_t^{in}(\theta_t) C_{pf}}{M_1 C_{pf}} & \dfrac{\dot{m}_t^{in}(\theta_t)}{M_1} \\ 0 & -\dfrac{A_2 U + \dot{m}_t^{in}(\theta_t) C_{pf}}{M_2 C_{pf}} \end{pmatrix}$
- $B = \begin{pmatrix} \dfrac{1}{M_1 C_{pf}} & 0 \\ 0 & \dfrac{1}{M_2 C_{pf}} \end{pmatrix}$

- $\bar{c}(\theta_t) = \left(\dfrac{A_1 U}{M_1 C_{pf}} x_{env}, \dfrac{A_2 U x_{env} + \dot{m}_t^{in}(\theta_t) C_{pf} x_{in}}{M_2 C_{pf}} \right)^T$

The thermal dynamics thus take the form

$$\frac{dx_t}{dt} = A(\theta_t)x_t + B\bar{u}_t + \bar{c}(\theta_t) \tag{2}$$

In the optimal control strategy detailed in Section 4, to keep the customers comfortable, we do not penalize the effort needed to maintain the EWH at its temperature at the start of the control horizon, but rather the effort needed to *deviate* from it when aiming for a different temperature. The thermal effort needed to remain on average at the initial temperature is thus obtained for free in our formulation, and $\bar{u}_{1,t}, \bar{u}_{2,t}$ can be written as follows:

$$\bar{u}_{1,t} = u_{1,t} \tag{2a}$$
$$\bar{u}_{2,t} = u_{1,t} + u_{2,t}^{free} \tag{2b}$$

with

$$u_{2,t}^{free} = UA_1(x_{1,0} - x_{env}) + UA_2(x_{2,0} - x_{env}) + E\left(\sum_{\theta_t \in \{1,2\}} \zeta_{\theta_t,\infty} \dot{m}_t^{in}(\theta_t) C_{pf}(x_{1,t} - x_{in,t}) \right) \tag{3}$$

Then, the thermal dynamics take the form

$$\frac{dx_t}{dt} = A(\theta_t)x_t + Bu_t + c(\theta_t) \tag{4}$$

where $c(\theta_t)$ is modified from (2) to account for the free effort.

4 MFG-based control strategy

Nomenclature

Parameters

x^{low}	Lower comfort temperature, i.e., minimum permissible mean temperature in EWH
x^{high}	Upper comfort temperature, i.e., maximum permissible mean temperature in EWH
N_{wh}	Number of EWHs
q^{x_0}	Cost coefficient
R	Cost matrix
A^j	Matrix $A(\theta_t)$ for $\theta_t = j$, $j \in \{0, 1\}$
c^j	Vector $c(\theta_t)$ for $\theta_t = j$, $j \in \{0, 1\}$
L	$= \begin{pmatrix} -\alpha_0 & \alpha_0 \\ \alpha_1 & -\alpha_1 \end{pmatrix}$; infinitesimal generator of Markov chain θ_t

Variables

$x_{i,t}$	Temperature vector of EWH i at time t
$\bar{u}_{i,t}$	Power input vector in EWH i at time t

The control strategy we implement was introduced in [16]. As mentioned earlier, it is based on MFG theory [10, 19]. We consider a homogeneous group of N EWHs with identical layer structure and water extraction statistics. Their mean temperature is to follow a target temperature of y. In this prescriptive game theoretic framework, a cost function is attributed to a generic individual EWH $i \in \{1, \cdots, N\}$ as follows:

$$\begin{aligned} J_i^N(u^i, j, t) =& E\left[\int_t^T \left[(Hx_{i,\tau} - z)^2 q_\tau^y + (Hx_{i,\tau} - Hx_{i,0})^2 q^{x_0}\right] d\tau | \theta_t = j\right] \\ &+ E\left[\int_t^T \left[||u_{i,\tau}||_R^2\right] d\tau + (Hx_{i,T} - z)^2 q_T^y + (Hx_{i,T} - Hx_{i,0})^2 q^{x_0} | \theta_t = j\right] \end{aligned} \tag{5}$$

where

- $q_t^y = \left|\lambda \int_0^t (H\bar{x}_\tau - y) d\tau\right|$;
- z is set to x^{low} if the objective is to decrease the mean aggregate temperature, and to x^{high} if the objective is to increase that temperature;
- $\bar{x}_t = \sum_{i=1}^N \frac{1}{N} x_{i,t}$ is the vector of mean temperatures of the group of EWHs;
- $H = \begin{pmatrix} \frac{1}{2} & \frac{1}{2} \end{pmatrix}$;
- $||u_{i,t}||_R^2 = (u_{i,t})^T R u_{i,t}$.

Let us remark that $x_{i,t}$ and $\bar{x}_t$ are vectors whose dimension is the number of layers in the tank. Thus, Hx_t^i is the mean water temperature in EWH i.

This formulation of the cost function is unusual in that the cost coefficient q_t^y generating the pressure to go toward z (first term on the RHS of (5)) is an *integral cost* depending on the deviation from the target. This means that the pressure (either to store energy or to decrease energy power consumption) continues to build up as long as the mean temperature has not reached the target temperature. This temperature change is partially countered by the second term on the RHS of (5), which penalizes deviations from the EWH's initial temperature. Thus, each EWH reaches its own specific steady-state with a mean temperature somewhere between the initial temperature and temperature z (ensuring local customer comfort), while the overall mean temperature for the set of EWHs reaches the target y. This happens while we minimize the relative temperature changes in each EWH. Furthermore, those EWHs that can contribute the most are subject to the highest pressure, and they contribute accordingly when we compute their best response policy.

When the number of controlled EWHs is large, the laws of large numbers dictate that the aggregate mean temperature vector $\bar{x}_t$ converges to a deterministic (but a priori unknown) trajectory. Because that trajectory no longer depends on the actions of individual EWHs, (5) can be viewed as an isolated EWH, leading to a classical optimal tracking problem [15]. Viewed as a tracking problem for a linear quadratic regulator, this problem can be solved through a system of Riccati equations with variables Π_t^j and offset variables $s_{i,t}^j$ [16].

This system can be used to compute the control we need to apply to each individual EWH to achieve the common goal of reaching the target temperature. The system depends on the unknown

q_t^y and to obtain it, we need to consider that *individuals that are optimally responding to the assumed q_t^y must collectively produce a mean temperature response $\bar{x}_t$ such it replicates the assumed q_t^y*. When this condition is fullfilled, one can claim that the Nash equilibrium of the game has been reached. The above argument implies that we need to find the fixed point of the following system:

$$q_t^y = \left| \lambda \int_0^t (H\bar{x}_\tau - y) d\tau \right| \tag{6a}$$

$$-\frac{d\Pi_t^0}{dt} = \Pi_t^0 A^0 + A^{0^T}\Pi_t^0 - \Pi_t^0 B R^{-1} B^T \Pi_t^0 - \alpha_0 \Pi_t^0 + \alpha_0 \Pi_t^1 + (q_t^y + q^{x_0}) H^T H \tag{6b}$$

$$\Pi_T^0 = (q_T^y + q^{x_0}) H^T H \tag{6c}$$

$$-\frac{d\Pi_t^1}{dt} = \Pi_t^1 A^1 + A^{1^T}\Pi_t^1 - \Pi_t^1 B R^{-1} B^T \Pi_t^1 + \alpha_1 \Pi_t^0 - \alpha_1 \Pi_t^1 + (q_t^y + q^{x_0}) H^T H \tag{6d}$$

$$\Pi_T^1 = (q_T^y + q^{x_0}) H^T H \tag{6e}$$

$$-\frac{ds_t^0}{dt} = (A^0 - B R^{-1} B^T \Pi_t^0)^T s_t^0 + \Pi_t^0 c^0 - (q_t^y z + q^{x_0} H \bar{x_0}) H^T - \alpha_0 s_t^0 + \alpha_0 s_t^1 \tag{6f}$$

$$s_T^0 = -(q_t^y z + q^{x_0} H \bar{x_0}) H^T \tag{6g}$$

$$-\frac{ds_t^1}{dt} = (A^1 - B R^{-1} B^T \Pi_t^1)^T s_t^1 + \Pi_t^1 c^1 - (q_t^y z + q^{x_0} H \bar{x_0}) H^T + \alpha_1 s_t^0 - \alpha_1 s_t^1 \tag{6h}$$

$$s_T^1 = -(q_t^y z + q^{x_0} H \bar{x_0}) H^T \tag{6i}$$

$$\frac{d\bar{x}_t^0}{dt} = (A^0 - B R^{-1} B^T \Pi_t^0)\bar{x}_t^0 - \alpha_0 \bar{x}_t^0 + \alpha_1 \bar{x}_t^1 + \zeta_{0,t} c^0 - \zeta_{0,t} B R^{-1} B^T s_t^0 \tag{6j}$$

$$\frac{d\bar{x}_t^1}{dt} = (A^1 - B R^{-1} B^T \Pi_t^1)\bar{x}_t^1 + \alpha_0 \bar{x}_t^0 - \alpha_1 \bar{x}_t^1 + \zeta_{1,t} c^1 - \zeta_{1,t} B R^{-1} B^T s_t^1 \tag{6k}$$

$$\bar{x}_t = \bar{x}_t^0 + \bar{x}_t^1 \tag{6l}$$

$$\bar{x}_t^0 = E(\mathbb{1}(\theta_t = 0)\bar{x}_t) \tag{6m}$$

$$\bar{x}_t^1 = E(\mathbb{1}(\theta_t = 1)\bar{x}_t) \tag{6n}$$

where $\zeta_t = [\zeta_{1,t}, \zeta_{,t}]$ is defined by

$$\frac{d\zeta_t}{dt} = \zeta_t L^T \tag{6o}$$

Computing the fixed point of (6) corresponds to finding the Nash equilibrium of the MFG. Then q_t^y can be used to find the individual control laws of each EWH. To simplify the solution process we used $\zeta_\infty = \left[\frac{\alpha_1}{\alpha_1+\alpha_0}, \frac{\alpha_0}{\alpha_1+\alpha_0}\right]$, the quasi steady-state probability of the Markov chain, instead of ζ_t. The algorithm used to find the fixed point is described in the next section.

5 Near-fixed-point framework

While under some technical conditions a fixed point always exists [16], it may not always be desirable, i.e., associated with a bounded q_t^y as t goes to infinity (or equivalently, a mean EWH temperature that converges to the target y). We instead look for a desirable near-fixed point such that the trajectory converges to y when $t \to \infty$, which means that the cost coefficient trajectory $q_t^y(\lambda)$ must converge to some q_∞^y satisfying the steady-state equation of (6) with $\bar{x}_\infty = y$. Since convergence to a fixed point with an iterative algorithm depends strongly on the choice of integration coefficient λ, we modify our approach relative to [16], inspired by the near-fixed-point calculations in [17], to rely on the solution of a suitable optimization problem.

Let $\mathcal{S}_\lambda(\bar{x}_t(\lambda))$ be the solution of (6) for mean temperature trajectory $\bar{x}_t$ and coefficient λ in the definition of q_t^y. We want to select the trajectory that is closest to a fixed point within a family of

mean trajectories $\bar{x}_t(\lambda)$ with the correct steady-state behavior. This family, first introduced in [17] for space heaters, is constructed as follows. Let $N_q > n_q > 1$ and $t_0 > 0$. We solve system (6) with the cost coefficient

$$q_t^y = \begin{cases} n_q q_\infty^y & \text{if } t \in [0, t_0] \\ q_\infty^y & \text{if } t \geq t_0 \end{cases}$$

to obtain $\bar{x}_{1,t}$ and with

$$q_t^y = \begin{cases} N_q q_\infty^y & \text{if } t \in [0, t_0] \\ q_\infty^y & \text{if } t \geq t_0 \end{cases}$$

to obtain $\bar{x}_{2,t}$. Although they may not be fixed points, these two trajectories satisfy the correct steady-state behavior and constitute the bounds of the family. The associated lambdas are

$$\lambda_1 = \frac{q_\infty^y}{\left|\int_0^\infty (H\bar{x}_\tau^1 - y)d\tau\right|} \text{ and } \lambda_2 = \frac{q_\infty^y}{\left|\int_0^\infty (H\bar{x}_\tau^2 - y)d\tau\right|}.$$

The family is then defined as

$$\mathcal{F}(f) = \{\bar{x}_t(\lambda) | \lambda = \frac{q_\infty^y}{\left|\int_0^\infty (H\bar{x}(\lambda)_\tau - y)d\tau\right|}, \bar{x}_t(\lambda) = f\bar{x}_{1,t} + (1-f)\bar{x}_{2,t},$$

$$f \in [0,1], \lambda \in [\min(\lambda_1, \lambda_2), \max(\lambda_1, \lambda_2)]\}.$$

Within this family, we select the trajectory that is the closest to a fixed point using the following optimization problem where the optimized variables are on n_q, N_q, t_0 and f:

$$\begin{aligned}
\min \quad & a_1 \overbrace{||\bar{x}_t(\lambda) - \mathcal{S}_\lambda(\bar{x}_t(\lambda))||_{\mathcal{L}_2}}^{\text{so as to be a fixed point}} + a_2 \overbrace{(\mathcal{S}_\lambda(\bar{x}_t(\lambda))(T) - y)^2}^{\text{convergence to the target}} && \text{(7a)} \\
\text{s.t.} \quad & \bar{x}_{1,t}, \lambda_1, \bar{x}_{2,t}, \lambda_2 \text{ computed as described above} && \text{(7b)} \\
& \bar{x}_t(\lambda) \in \mathcal{F}(f) && \text{(7c)} \\
& N_q \in [1, N_q^{max}] && \text{(7d)} \\
& n_q \in [1, n_q^{max}] && \text{(7e)} \\
& t_0 \in [0, t_0^{max}] && \text{(7f)}
\end{aligned}$$

where N_q^{max}, n_q^{max} and t_0^{max} are chosen arbitrarily: we set them to (4,2,5).

The choice of the length of the control horizon T and of n_q and N_q allows us to regulate somewhat the speed at which we wish the aggregate control to operate. The resulting optimal trajectory $\bar{x}_t$ may be sent by the aggregator to all EWHs so that they implement locally their optimal control policy. Alternatively, if local computational capacity permits, the optimization can be carried out locally by each EWH with only the aggregate mean temperature vector communicated at the start of the control horizon.

6 Assessment of potential flexibility product offer based on macroscopic-level EWH model

Nomenclature

Parameters

x_{env}	Temperature of surroundings
x_{in}	Inlet fluid temperature

x^{low}	Lower comfort temperature
x^{high}	Upper comfort temperature
C_{pf}	Specific heat of fluid
U	Loss coefficient between tank and surroundings
ρ	Water density
V	EWH volume
A	EWH surface area
$\dot{V}^{mix}$	Water flow of extraction
$\dot{Q}$	Maximum power of the heating elements, equal to $\sum_i \dot{Q}_i$, the sum of the maximum power of the heating elements of the individual EWHs.
N_{wh}	Number of EWHs
Δ_t	Time discretization step
T_{start}	Time at which control of EWHs starts
T_{end}	Time at which control of EWHs stops
T_1	Time dividing the control horizon: on each interval the objective is slightly different (see Figure 2)
$t_{rebound}$	Duration of constraint on size of post-control rebound
$r_{rebound}$	Acceptable range for post-control rebound as percentage of base load
d_t	Uncontrolled demand at time t
p_t^b	Base aggregate EWH power demand at time t
x_{mix}	Temperature desired by customer
$\zeta_{j,\infty}(t)$	Quasi steady-state probability of state j of the water extraction Markov chain associated with the infinitesimal generator L_t defined by $\zeta_\infty(t) = \left[\frac{\alpha_1}{\alpha_1+\alpha_0}, \frac{\alpha_0}{\alpha_1+\alpha_0}\right]$
$C_{direction}$	Indicator for increase (+1) or decrease (-1) in power consumption
c_d	Integer coefficient in a bisection-type search

Variables

p_t^s	Simulated aggregated EWH power demand
φ_t^{max}	Upper bound on energy to inject into EWH on interval $[t, t+\Delta_t]$
$\boldsymbol{\varphi^{max}}$	$= (\varphi^{max}_{T_{start}}, \cdots, \varphi^{max}_t, \cdots, \varphi^{max}_{T_{end}})$
$\boldsymbol{\varphi^{max}_{prev}}$	Upper bound vector in bisection-based algorithm applied to the bounds of the energy to inject into EWH: equals $(\varphi^{max}_{prev,T_{start}}, \cdots, \varphi^{max}_{prev,t}, \cdots, \varphi^{max}_{prev,T_{end}})$
φ_t^{min}	Lower bound on energy to inject into EWH on interval $[t, t+\Delta_t]$
$\boldsymbol{\varphi^{min}}$	$= (\varphi^{min}_{T_{start}}, \cdots, \varphi^{min}_t, \cdots, \varphi^{min}_{T_{end}})$
$\boldsymbol{\varphi^{min}_{prev}}$	Lower bound vector in bisection-based algorithm applied to the bounds of the energy to inject into EWH: equals $(\varphi^{min}_{prev,T_{start}}, \cdots, \varphi^{min}_{prev,t}, \cdots, \varphi^{min}_{prev,T_{end}})$

Decision variables

e_t	Energy stored in EWHs at time t
φ_t	Energy to inject into EWHs on interval $[t, t+\Delta_t]$
w_t	Intermediary variable used to penalize variability in power demand

In this section we describe how to determine the maximum increase/decrease in the power consumption that the aggregator is able to achieve with a given set of EWHs given the constraints on the rebound size guaranteed in the proposed flexibility product. This information is then used in the MFG-based approach from Section 5 to determine the target temperatures.

At the macroscopic level, and for aggregator planning purposes, recall that we model the set of EWHs as *one massive aggregated EWH*, with insulation characteristics identical to those of the individual EWHs, a volume equal to the sum of their volumes, a single perfectly mixed layer, and a unique heating element with power rating equal to the sum of the individual power ratings. Subsequently, an energy balance analysis allows us to find the maximum amount of energy that can be injected into this aggregate EWH during a given Δ_t. We use a single-layer EWH for the aggregate model since only the determination of the mean temperature is relevant for the determination of the control of the individual EWHs. As discussed in Section 3, the individual EWHs are modeled with a two-layer model. The stored energy can then be converted into a target temperature for the mean field control using the equation

$$y_t = \frac{e_t}{N_{wh}\rho C_{pf}} + x_{env}.$$

Two conditions need to be satisfied. First, the EWH power demand must be as close as possible to constant during the control horizon. Second, the percentage rebound relative to the no-control base case beyond the end of the horizon must lie within an acceptable range, denoted $r_{rebound}$ and defined as a percentage deviation from the base power demand of the EWHs. This second condition guarantees that the action of the aggregator does not have unwanted consequences in the post-control period. The time intervals and objectives of our flexibility product are summarized in Figure 2.

To find the maximum achievable flexibility under the two conditions, we developed an algorithm with four blocks. The first is a *scheduler* that computes a temperature schedule depending on the bounds on the injected energy φ_t for $t \in [T_{start}, T_{end}]$: $\boldsymbol{\varphi^{min}} = (\varphi^{min}_{T_{start}}, \varphi^{min}_{T_{start}+\Delta_t}, \cdots, \varphi^{min}_{T_{end}})$ and $\boldsymbol{\varphi^{max}} = (\varphi^{max}_{T_{start}}, \varphi^{max}_{T_{start}+\Delta_t}, \cdots, \varphi^{max}_{T_{end}})$. The initial values of these vectors are $\boldsymbol{\varphi^{min}_{init}} = (0, 0, \cdots, 0)$ and $\boldsymbol{\varphi^{max}_{init}} = (\dot{Q}\Delta_t N_{wh}, \cdots, \dot{Q}\Delta_t N_{wh})$. The second block is a *Simulator* that performs a Monte Carlo simulation of N_{wh} water heaters under the temperature schedule computed at the current iteration, the control described in Section 4 and the dynamics described in Section 3. The third block is an *Updater* that determines the value of the bounds $\boldsymbol{\varphi^{min}}$, $\boldsymbol{\varphi^{max}}$ depending on whether or not the rebound constraint is satisfied. The last block is the *Convergence test* that determines whether we return to the first block or exit the algorithm. Figure 3 presents the flowchart.

6.1 Scheduler

The scheduler is based on linear programming and outputs a temperature schedule for the mean field controller.

Objective function to maximize

$$\begin{aligned} Obj(\varphi_t, z_t, t \in [T_{start}, T_{end}]) = a_1 \sum_{t \in]T_{start}, T_{end}]} C_{direction}(p^b_t - p_t) \\ - a_2 \sum_{t \in]T_{start}, T_1[} w_t - a_3 \sum_{t \in [T_1, T_{end}]} w_t \end{aligned}$$

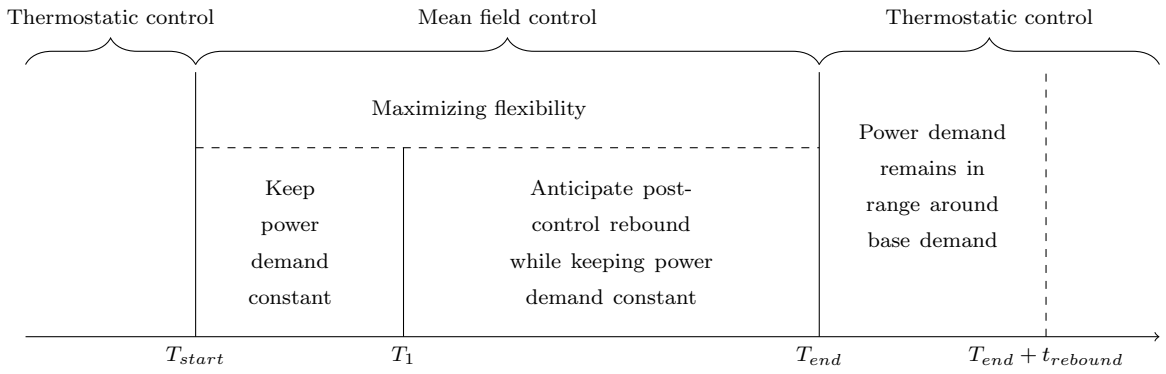

Figure 2: Specification of the differing objectives used over time to manage the post-control rebound.

The first term maximizes the mean increase/decrease in power demand relative to the base (i.e., uncontrolled) power demand, while the second and third terms penalize the variability in the control power demand in the two time periods.

Constraints

- The residential power consumption at each time step is the sum of the uncontrollable part d_t and the controllable part, namely the amount of power injected into the EWH:

$$p_t = d_t + \frac{\varphi_t}{\Delta_t}$$

- w_t is an intermediary variable that captures an upper bound on $|p_t - p_{t-1}|$ to be subsequently penalized as part of the cost:

$$\begin{aligned} w_t &\geq p_t - p_{t-1} \\ w_t &\geq p_{t-1} - p_t \end{aligned}$$

- The energy stored in the water heater at time t is equal to the amount of energy stored at $t-1$ plus the energy injected minus the losses:

$$\begin{aligned} e_t &= e_{t-1} + \varphi_t - l(e_{t-1}) \\ l(e_t) &= l_c(e_t) + l_{extr}(t) \end{aligned}$$

where

$$\begin{aligned} l_c(e_t) &= UA\left(\frac{e_t}{C_{pf}\rho V} + N_{wh}(x_{in} - x_{env})\right) \\ l_{extr}(t) &= \rho C_{pf}(x_{mix} - x_{in})V^{extract}(t) \\ V^{extract}(t) &= \sum_{j\in\{1,2\}} N_{wh}\zeta_{j,\infty}(t)\dot{V}_j^{mix}\Delta_t \end{aligned}$$

$l_c(e_t)$ corresponds to the loss from heat transfer by conduction with the environnement, $l_e(t)$ is the energy loss due to the water extraction, and $V^{extract}(t)$ represents the mean volume of water drawn for the aggregated EWH.

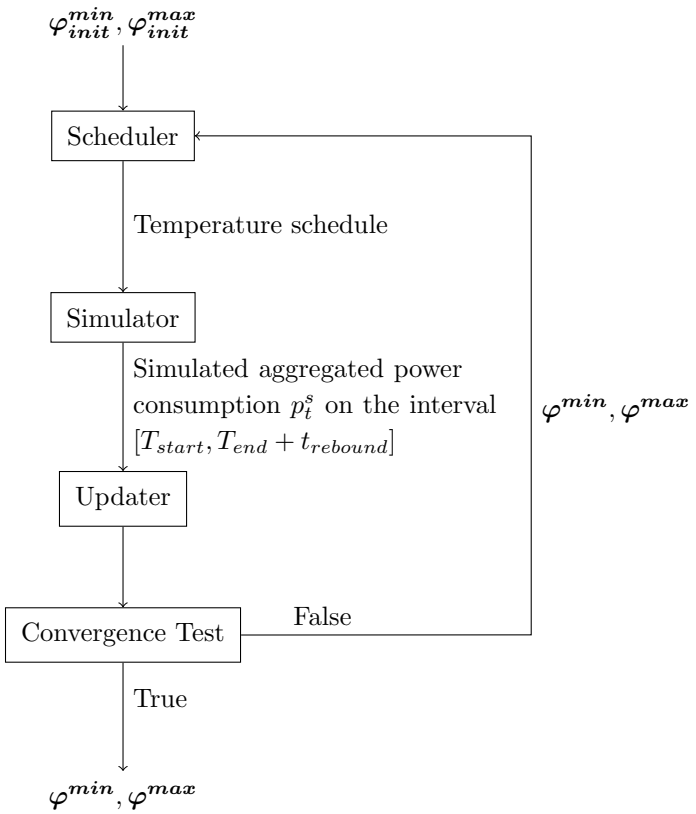

Figure 3: Flowchart for algorithm that determines the maximum flexibility at the macroscopic level.

- The energy stored in the EWH is linked to the temperature:

$$\begin{aligned} e_{T_{start}} &= N_{wh}\rho V C_{pf}(x_{init} - x_{in}) \\ e_t &\geq N_{wh}\rho V C_{pf}(x_{low} - x_{in}) \\ e_t &\leq N_{wh}\rho V C_{pf}(x_{high} - x_{in}) \end{aligned}$$

  This gives bounds on the energy we are able to store, depending on the initial amount of energy stored.

- The amount of energy that can be injected into the EWH is bounded below and above by the components of φ^{min} and φ^{max} at each time step. $B_{down}(t)$ and $B_{up}(t)$ in (8c) and (8d) below are active depending on the value of $C_{direction}$ and prevent overshooting/undershooting the initial temperature as we act to decrease/increase the power consumption; φ_t is bounded above/below accordingly:

$$\begin{aligned} \varphi_t &\geq \varphi_t^{min} && \text{(8a)} \\ \varphi_t &\leq \varphi_t^{max} && \text{(8b)} \\ \varphi_t &\geq B_{down}(t-1) && \text{(8c)} \\ \varphi_t &\leq B_{up}(t-1) && \text{(8d)} \end{aligned}$$

where

$$
\begin{aligned}
B_{down}(t) &= N_{wh}\rho V C_{pf}(C_+ x_{low} + C_- x_{init} - x_{in}) - e_t + l_t \\
B_{up}(t) &= N_{wh}\rho V C_{pf}(C_- x_{high} + C_+ x_{init} - x_{in}) - e_t + l_t \\
C_+ &= \frac{(1 + C_{direction})}{2} \\
C_- &= \frac{(1 - C_{direction})}{2}
\end{aligned}
$$

6.2 Simulator

The *Simulator* performs the simulation of the N_{wh} water heaters individually under the temperature schedule computed by the *Scheduler* through a Monte-Carlo simulation on the horizon $[T_{start} - 2h, T_{end} + t_{rebound}]$. We use simulation because the power demand during the rebound phase after T_{end}, needed to evaluate the rebound value, depends on the temperature distributions within the EWHs, and these distributions cannot be obtained from an aggregate model. Monte-Carlo simulation is needed because the temperature distribution depends on the individual end-use water demand Markov chain processes. Note that the simulation corresponds to standard thermostatic control until T_{start}, then moves to MFG-based control until T_{end}, at which point thermostatic control resumes. At T_{end}, EWHs with a cold mean temperature (below x_{low}) are set to an ON state, and all others are set to the OFF state.

6.3 Updater

The *Updater* takes as input the aggregated power demand computed by the *Simulator* p_t^s, p_t^b and $r_{rebound}$.

First, the *Updater* performs a rebound constraint test:

1. If $|p_t^s - p_t^b| \geq r_{rebound} p_t^b$, the rebound constraint is not satisfied;
2. If $|p_t^s - p_t^b| \leq r_{rebound} p_t^b$, the rebound constraint is satisfied.

Then, using a technique similar to bisection, it updates the bounds:

$$\boldsymbol{\varphi^{min}} = (\varphi^{min}_{T_{start}}, \varphi^{min}_{T_{start}+\Delta_t}, \cdots, \varphi^{min}_{T_{end}}) \text{ and } \boldsymbol{\varphi^{max}} = (\varphi^{max}_{T_{start}}, \varphi^{max}_{T_{start}+\Delta_t}, \cdots, \varphi^{max}_{T_{end}})$$

Only the last term of the vectors needs to be changed by the algorithm. Indeed, we then regulate the amount of energy to be injected into the tank on the last interval, to correct the size of the upcoming rebound. This has a ripple effect on the other components of the $\boldsymbol{\varphi_{min}}$ and $\boldsymbol{\varphi_{max}}$ vectors through constraints (8c) and (8d).

- If we are in case 1, the bounds are too permissive. They are updated as follows:
  - If $C_{direction} = 1$: $\boldsymbol{\varphi^{max}_{prev}} = \boldsymbol{\varphi^{max}}$ and $\varphi^{max}_{T_{end}} = \dfrac{(c_d - 1)\varphi^{max}_{T_{end}} + \varphi^{min}_{prev,T_{end}}}{c_d}$
  - If $C_{direction} = -1$: $\boldsymbol{\varphi^{min}_{prev}} = \boldsymbol{\varphi^{min}}$ and $\varphi^{min}_{T_{end}} = \dfrac{\varphi^{max}_{prev,T_{end}} + (c_d - 1)\varphi^{min}_{T_{end}}}{c_d}$
- If we are in case 2, the bounds may not be permissive enough. They are updated as follows:
  - If $C_{direction} = 1$: $\boldsymbol{\varphi^{min}_{prev}} = \boldsymbol{\varphi^{max}}$ and $\varphi^{max}_{T_{end}} = \dfrac{(c_d - 1)\varphi^{max}_{T_{end}} + \varphi^{max}_{prev,T_{end}}}{c_d}$

– If $C_{direction} = -1$: $\boldsymbol{\varphi^{max}_{prev}} = \boldsymbol{\varphi^{min}}$ and $\varphi^{min}_{T_{end}} = \dfrac{\varphi^{min}_{T_{end}} + (c_d - 1)\varphi^{min}_{prev,T_{end}}}{c_d}$

$\boldsymbol{\varphi^{min}_{prev}}$ and $\boldsymbol{\varphi^{max}_{prev}}$ are initialized with $\boldsymbol{\varphi^{min}_{init}}$ and $\boldsymbol{\varphi^{max}_{init}}$. The value of c_d can be set to 2 or to say 10 or 50 if we want a slower variation in the bounds (since the variation of the rebound is not monotone, a slower change may be desirable to avoid missing the minimum rebound).

We observe that acting on $\varphi^{max}_{T_{end}}, \varphi^{min}_{T_{end}}$ will lead to a corresponding change in the temperature schedule. The last target of the schedule will follow the same trend as $\varphi^{max}_{T_{end}}, \varphi^{min}_{T_{end}}$. For example, a decrease/increase of $\varphi^{max}_{T_{end}}/\varphi^{min}_{T_{end}}$ will result in a decrease/increase of the last target temperature. Combining this with the last term of the objective function, which ensures that the power consumption remains as constant as possible on $[T_1, T_{end}]$, we expect that the target temperature will gradually increase or decrease on $[T_1, T_{end}]$ to prepare the EWHs to shift to thermostatic control and anticipate the post-control rebound. The case study in Section 7 confirms this.

6.4 Convergence Test

We exit the algorithm if $C_+|\varphi^{max}_{prev,T_{end}} - \varphi^{max}_{T_{end}}| + C_-|\varphi^{min}_{prev,T_{end}} - \varphi^{min}_{T_{end}}|$ is small enough or when we reach the maximum number of iterations, where $C_+ = \dfrac{(1 + C_{direction})}{2}$ and $C_- = \dfrac{(1 - C_{direction})}{2}$.

7 Case Study

Nomenclature

Parameters

$N_w h$	Number of EWHs (i.e., clients)
T_{start}	Time at which control of EWHs starts
T_{end}	Time at which control of EWHs stops
$t_{rebound}$	Duration of post-control rebound check
$r_{rebound}$	Acceptable range for post-control rebound
$\bar{c}_W$	Mean value deviation of controlled power demand from base power demand over $[T_{start}, T_{end}]$; negative for a load reduction and positive for a load increase
C_{eq}	Auction clearing price
$C_i^{control}$	Price paid by client i when MFG control is applied
C_i^{base}	Price paid by client i when no control is applied
F_i	Net cash flow of month i
I	Initial investment
a	Discount rate

We use the setup of the SMARTDesc project [31]. We consider 500 identical EWHs with a two-layer tank. The infinitesimal generator L_t of the Markov chain modeling water extraction is piecewise constant every 2 h during the day, with the values taken from [32]. The Markov chain has two states $\theta_t \in \{0, 1\}$ that represent the absence or presence of water extraction, and $\dot{m}_t = \dot{V}^{mix}\theta_t$ where $\dot{V}^{mix} = 2.62\,\ell/\text{min}$ is the extraction flow. Table 1 gives the parameter values.

We ran the scheduler described in Section 6 with $T_1 = T_{start} + 2\,h$ and $T_{end} = T_{start} + 4\,h$, i.e., the EWHs are controlled for four hours, with flexibility maximization for the first two hours, and anticipation of the post-control rebound during the remaining time. Then we constrained

Table 1: Parameter values for simulations

$\dot{Q}_i$	$4500\,W$	A	$2.55\,m^2$
x_{env}	$25°C$	M_l	$136.5\,kg$
x_{in}	$15°C$	C_{pf}	$4190\,J/(kgK)$
x^{low}	$50°C$	U	$28.38 J/(m^2 K min)$
x^{high}	$60°C$	$\dot{V}_j^{mix}$	$2.62\,l/min$
x_{mix}	$38°C$	q^{x_0}	$8000\,h^{-1}$
V	$273\,\ell$	R	$\begin{pmatrix} 0.025 & 0 \\ 0 & 0.025 \end{pmatrix} h^{-1}$

the modified power demand to remain in the interval limits around the base power demand for $t_{rebound} = 2\,h$. All the computations were carried out on a `Intel(R) Core(TM) i7-2600 CPU @ 3.40 GHz` with eight processors. The results are reported in Figures 5 and 6.

The total power consumption considered is that of 500 homes and represents the sum of the uncontrollable demand, d_t, and that of the 500 EWHs simulated independently with distinct initial conditions and extraction trajectories. This corresponds to Monte Carlo simulations of 500 EWHs with the parameters given in Table 1. The base power demand with which our simulations are compared is the total power consumption of the 500 homes. The power demand data are taken from the public-demand data of the Independent Electricity System Operator (IESO) of Ontario, Canada [12]. We used the data from January 30, 2019. This data represents the overall power demand; we applied a reduction coefficient, 10^{-4}, to obtain the power consumption for 500 homes. Figure 4 shows the evolution of the parameter values of the hot water demand Markov chain over the day.

We consider two cases:

- Case 1: Active control between 7:00 and 11:00. This consists of a two-hour period of power reduction relative to base power demand, then two hours to anticipate the rebound; after 11:00 the mean field control ends and we revert to classical thermostatic control.

- Case 2: Active control between 14:00 and 18:00. This consists of a two-hour period of power increase relative to base power demand, then two hours to anticipate the rebound; after 18:00 we revert to classical thermostatic control.

Figures 5 and 6 show the output of our optimization for the two cases. The results are very similar. The target temperature schedules (Figures 5a and 6a) show that on the first part of the control period (before T_1) the strategy is to have a target temperature that decreases (resp. increases). After T_1 the target starts to increase (resp. decrease) again to heat (resp. cool) the EWHs gradually to anticipate the rebound and keep the temperature distribution away from the comfort bounds. Figures 5b and 6b show that while achieving the objective of decreasing (resp. increasing) the power demand, the rebound stays within a 9% range (resp. 14% range) of the base power consumption. This percentage is part of the specification of the flexibility product, and it can be tailored to the needs of the utility.

Figures 5a and 6a show that the simulated mean temperatures of the 500 EWHs do not reach the target temperatures in the decreasing-temperature phase whereas in the increasing-temperature phase they are closer to the target temperatures. This is because in the cooling phase the EWHs need more time to reach the target temperatures, and 15 minutes is not enough.

In case 2, we reach the comfort upper bound. So if the initial temperature were lower, we expect that we could have had more flexibility, as we could have increased the temperature more.

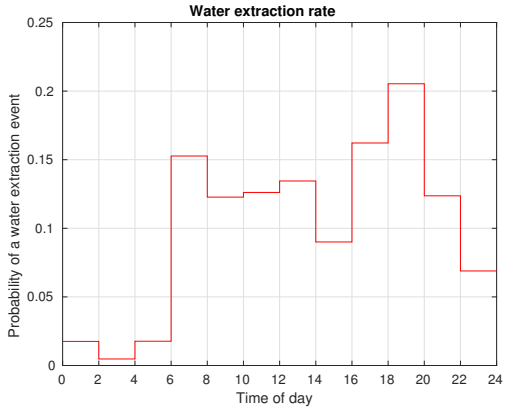

(a) Steady-state probability of water extraction event

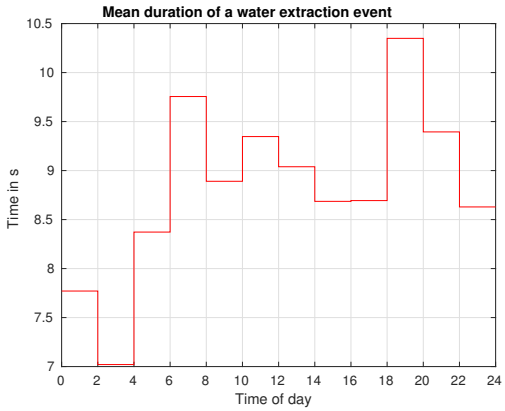

(b) Mean duration of water extraction events

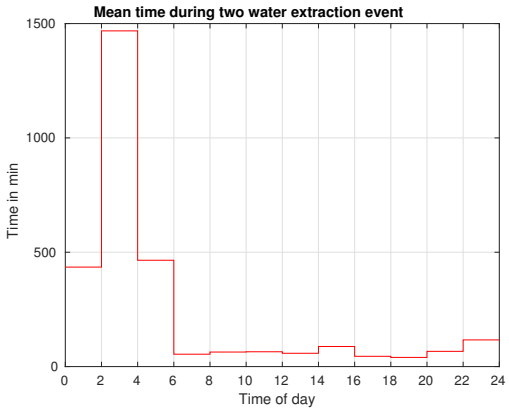

(c) Mean time between two water extraction events

Figure 4: Evolution of the parameters of the Markov chain during the day.

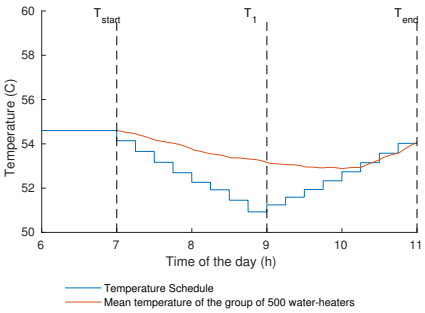

(a) Mean field target schedule temperature

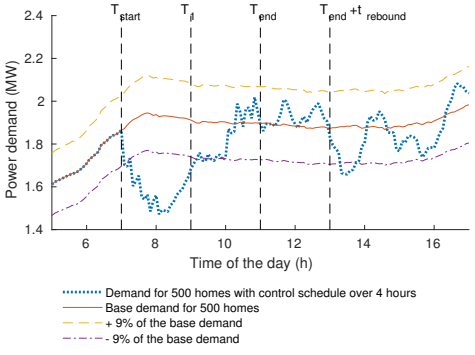

(b) Comparison of baseline power demand and the power demand under the schedule in Figure 5a

Figure 5: Case 1: Decrease of the power demand.

An initial phase during which we decrease the temperature of the EWHs, to anticipate our need for flexibility, could then be beneficial. The converse will be true in a situation where a power decrease is needed.

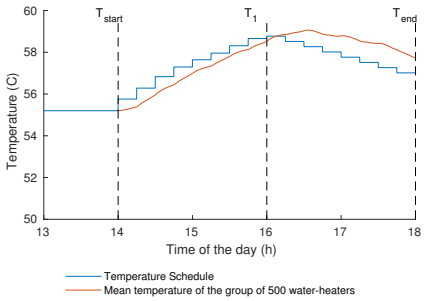

(a) Mean field target schedule temperature

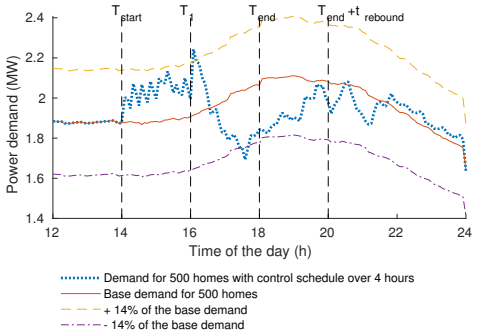

(b) Comparison of baseline power demand and the power demand under the schedule in Figure 6a

Figure 6: Case 2: Increase of the power demand.

The assumption of piecewise constant statistics for the hot-water-demand Markov chain leads to some simulation issues. Figure 4b shows that the steady-state probability of water extraction can undergo huge variations at certain hours (6:00 or 14:00 for example), and this has an impact on the simulation as we can see in Figure 7. Figure 7a shows that at 14:00 there is an unwanted drop in the power demand that is linked to the sudden changes in the Markov chain statistics. Similarly, we observe an unexpected increase in Figure 7b at 6:00. These side effects likely have two sources. First, in equation (6) we used the steady-state probability ζ_{∞}^{j} instead of the transient probability ζ_{t}^{j} to simplify the solution. Second, for analysis and model identification reasons, we used a model of the hot-water-demand Markov chain associated with piecewise constant statistics instead of a more realistic model with continuously changing statistics.

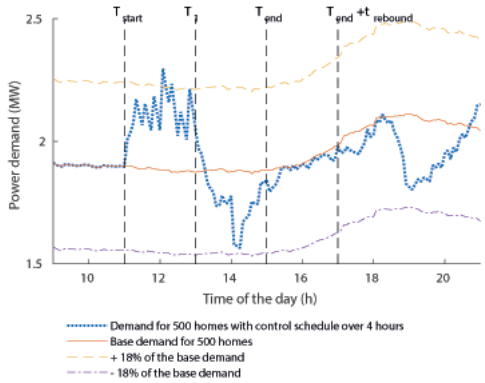

(a) Power demand of the group of EWHs with 14:00 in the control interval

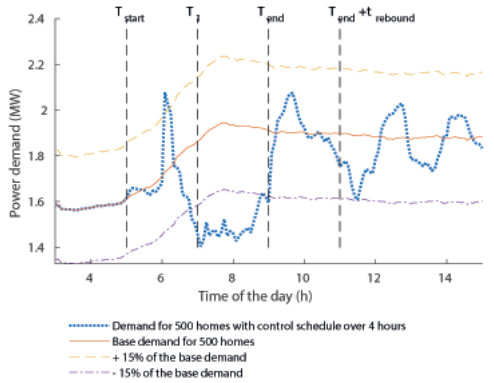

(b) Power demand of the group of EWHs with 6:00 in the control interval

Figure 7: Simulation artefacts due to discontinuities in hot-water demand.

Recall that the main constraint added in this work is that post-load-control deviations from the base behavior should remain within predefined bounds that are part of the flexibility product specification. However, in cases such as that shown in Figure 8, such deviation can be beneficial since it results in a decrease of the evening peak demand. This indicates that constraints on the

post-load-control deviations should depend in general on the operator's goals.

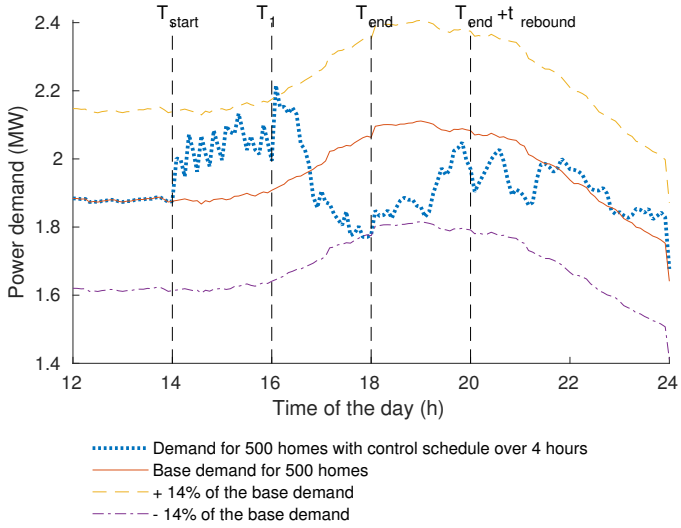

Figure 8: Flexibility offer with beneficial oscillation.

Financial assessment

To assess the economic viability of aggregation we consider the case of Ontario (Canada) with the Ontario time-of-use (TOU) prices; all figures are given in Canadian dollars. TOU prices [25] are used to measure the impact of flexibility control. The financial incentives given to participating customers should be 0 if they pay less when the control is applied or the net cost of the flexibility action if they pay more. We next need to evaluate for how much the aggregator can sell their flexibility on the market. For this we rely on the *Auction clearing price* of the Demand Response Auction in Ontario [12]. In this auction, bidders commit to providing flexibility for every business day of a six-month period. Given these two quantities, we can evaluate the profit for the aggregator for each flexibility product. Table 2 summarizes the results for cases 1 and 2. The profit equation is as follows:

$$Profit = \overbrace{C_{eq} \times \bar{c}_W}^{\text{Product billing}} - \overbrace{\sum_{i=1}^{N_{wh}} min(0, C_i^{control} - C_i^{base})}^{\text{Incentives to consumers}} \tag{9}$$

We next perform a net present value (NPV) study for an EWH aggregator, with the following formula:

$$NPV(T) = \sum_{i=0}^{T} \frac{F_i}{(1+a)^i} - I \tag{10}$$

We consider that the initial investment I is the cost of purchase of new EWHs for the 500 homes, with an average cost of \$425 each. The lifetime is expected to be 10 to 15 years, so T is set to 120 or 180 months. The net cash flow each month, F_i, is the profit obtained from the combination of the two flexibility offers (cases 1 and 2) every day, and we consider a discount rate, a, of 6% per year, or 0.49% per month [14]. Table 3 gives the results of this study. With a participation of

40% from the aggregator, the NPV becomes positive in 5 years, and with a 50% participation, it becomes positive in 7.5 years. This type of investment seems to be profitable with a participation rate below 40% to 50%, taking into account the lifetime of an EWH. Keeping in mind that the outcome of the financial assessment strongly depends on the assumptions and flexibility offer made, this simple study suggests that an investment of more than 50% of the price of a new EWH would not be profitable. More detailed studies should be carried out in the future, and in particular, the dependence of the participation rates on the incentives provided should be carefully assessed.

Table 2: Profit from sale of flexibility on market for Cases 1 and 2

Case	Duration	Rebound Percentage	$\bar{c}_W$ in kW on $[T_{start}, T_{end}]$	Profit (CAD)
1	4	9%	203	47.6
2	4	14%	27	6.3

Table 3: Net present value after 10 years and 15 years given different participation rates and profitability times

Discount rate	Participation (%)	Profitability time (months)	NPV in CAD (10 y)	NPV in CAD (15 y)
0.49%	100	–	-65 798	-18 915
0.49%	50	80	40 451	87 334
0.49%	40	61	61 701	108 584
0.49%	30	44	82 951	129 834
0.49%	0	0	146 701	193 584

8 Conclusion

In this paper, we have proposed a flexibility product for a water heater aggregator. The control strategy used for the water heaters is a mean field approach that is suited for controlling large-scale groups. We have adapted a recently developed strategy [17] for solving the mean field control problem for space-heaters to the case of water heaters. More precisely, we used an optimization approach to find a trajectory for the water heaters to follow as an approximate mean field control strategy that is guaranteed to meet the target. Then, to assess the possible flexibility that the group of water heaters could provide during a fixed interval, we used a linear program that works as a target scheduler for the mean field controller. The output is a schedule that maximizes the flexibility provided. To incorporate an additional constraint that ensures that the rebound, at the end of the control period, is limited compared to the base power consumption, we added a bisection-like algorithm to iterate on possible temperature schedules and find eligible schedules. This algorithm allows the aggregator to evaluate the possible flexibility that it can offer for its group of water heaters, the flexibility product being defined by:

- the time interval for application of the aggregator control, $[T_{start}, T_{end}]$;
- the mean deviation of the modified power demand from the base demand over $[T_{start}, T_{end}]$;
- the allowed percentage of deviation from the base demand in the post-control period;

- the duration of the post-control period.

The proposed algorithms have limitations. One is the computational time required: Optimization packages are relatively slow in solving (7) to determine a specific optimal mean temperature trajectory. In particular, to simulate the detailed behavior of a collection of water heaters for a given planned mean temperature trajectory with the scheduler, we need a total of $\frac{T_{end} - T_{start}}{\Delta_t}$ trajectories. The solvers used in this project take 30 s on average to compute one trajectory, which means that for a 4 h control with 15 min time steps, it takes more than 480 s (8 min) to obtain a complete temperature plan. In addition, to find an acceptable temperature plan for a given rebound percentage, it is necessary to simulate several plans, and the computing time becomes fairly long.

The second limitation is that our analysis is deterministic: the base power of the controlled water heaters and the rest of the uncontrolled user demand are considered to be known over the control horizon whereas in reality they are stochastic quantities. This limitation is more serious in the presence of renewable sources of generation.

In future work, it would be interesting to consider stochastic approaches for the scheduler to take into account the uncertainty on both the production of renewable sources and on the water extraction statistics. This would result in a more robust schedule. It could also be of interest to develop a specific near-fixed-point solver that could exploit the form of the optimization problem for greater efficiency. Finally, more detailed economic modelling could give more reliable information on the profitability of the activities of aggregators.

Acknowledgment

This work was supported by the NSERC Energy Storage Technology (NEST) Network and by the Group for Research in Decision Analysis (GERAD).

References

[1] X. Ayón, J.K. Gruber, B.P. Hayes, J. Usaola, and M. Prodanović. An optimal day-ahead load scheduling approach based on the flexibility of aggregate demands. Applied Energy, 198:1–11, 2017.

[2] Mattia Barbero, Cristina Corchero, Lluc Canals Casals, Lucia Igualada, and F.-Javier Heredia. Critical evaluation of European balancing markets to enable the participation of demand aggregators. Applied Energy, 264:114707, 2020.

[3] S. M. Basnet, H. Aburub, and W. Jewell. Effect of demand response on residential energy efficiency with direct load control and dynamic price control. In 2015 IEEE Eindhoven PowerTech, pages 1–6, 2015.

[4] Carlos Adrian Correa-Florez, Andrea Michiorri, and Georges Kariniotakis. Robust optimization for day-ahead market participation of smart-home aggregators. Applied Energy, 229:433–445, 2018.

[5] C. Eid, P. Codani, Y. Chen, Y. Perez, and R. Hakvoort. Aggregation of demand side flexibility in a smart grid: A review for European market design. In 2015 12th International Conference on the European Energy Market (EEM), pages 1–5, 2015.

[6] L. Gkatzikis, I. Koutsopoulos, and T. Salonidis. The role of aggregators in smart grid demand response markets. IEEE Journal on Selected Areas in Communications, 31(7):1247–1257, 2013.

[7] Gouvernement du Québec. Politique Énergétique du Québec, 2016. [Accessed: April 2018].

[8] Justin Gundlach and Romany Webb. Distributed Energy Resource Participation in Wholesale Markets: Lessons from the California ISO. Energy Law Journal, 39(1):47–77, May 2018.

[9] Eric Hsieh and Robert Anderson. Grid flexibility: The quiet revolution. The Electricity Journal, 30(2):1–8, March 2017.

[10] M. Huang, R. P Malhamé, and P. E Caines. Large population stochastic dynamic games: Closed-loop Mckean-Vlasov systems and the Nash certainty equivalence principle. Communications in Information & Systems, 6(3):221–252, 2006.

[11] IESO. Demand Response Auction in Ontario, 2019. [Accessed: February 2019].

[12] IESO. Power Data - Data Directory, 2019. [Accessed: February 2019].

[13] José Iria, Filipe Soares, and Manuel Matos. Optimal supply and demand bidding strategy for an aggregator of small prosumers. Applied Energy, 213:658–669, 2018.

[14] Jean-René Tagne Kuelah. L'évaluation du rendement d'une dépense publique, 2016. [Accessed: June 2019].

[15] D.E. Kirk. Optimal Control Theory: An Introduction. Dover Books on Electrical Engineering Series. Dover Publications, 2004.

[16] A.C. Kizilkale and R.P. Malhamé. Chapter 20 - Collective target tracking mean field control for Markovian jump-driven models of electric water heating loads. In Kyriakos G. Vamvoudakis and Sarangapani Jagannathan, editors, Control of Complex Systems, pages 559–584. Butterworth-Heinemann, 2016.

[17] Arman C. Kizilkale, Rabih Salhab, and Roland P. Malhamé. An integral control formulation of mean field game based large scale coordination of loads in smart grids. Automatica, 100:312–322, 2019.

[18] E. Koliou, C. Eid, J. P. Chaves-Ávila, and R. A. Hakvoort. Demand response in liberalized electricity markets: Analysis of aggregated load participation in the German balancing mechanism. Energy, 71:245–254, 2014.

[19] J.-M. Lasry and P.-L. Lions. Jeux à champ moyen. II–horizon fini et contrôle optimal. Comptes Rendus Mathématique, 343(10):679–684, 2006.

[20] A. Mahmood, A. R. Butt, U. Mussadiq, R. Nawaz, R. Zafar, and S. Razzaq. Energy sharing and management for prosumers in smart grid with integration of storage system. In 2017 5th International Istanbul Smart Grid and Cities Congress and Fair (ICSG), pages 153–156, 2017.

[21] Filippo Malandra, Arman C. Kizilkale, Frédéric Sirois, Brunilde Sansò, Miguel F. Anjos, Michel Bernier, et al. Smart distributed energy storage controller (smartDESC). Technical Report G-2020-15, 2020, Cahiers du GERAD.

[22] Roland Malhamé. A jump-driven Markovian electric load model. Advances in Applied Probability, 22(3):564–586, 1990.

[23] A. Mohsenian-Rad, V. W. S. Wong, J. Jatskevich, R. Schober, and A. Leon-Garcia. Autonomous demand-side management based on game-theoretic energy consumption scheduling for the future smart grid. IEEE Transactions on Smart Grid, 1(3):320–331, 2010.

[24] F.L. Müller and B. Jansen. Large-scale demonstration of precise demand response provided by residential heat pumps. Applied Energy, 239:836–845, 2019.

[25] Ontario Hydro. Ontario TOU prices, 2019. [Accessed: February 2019].

[26] Guangsheng Pan, Wei Gu, Zhi Wu, Yuping Lu, and Shuai Lu. Optimal design and operation of multi-energy system with load aggregator considering nodal energy prices. Applied Energy, 239:280–295, 2019.

[27] Ignacio Pérez-Arriaga and Christopher Knittel. Utility of the Future. Technical report, MIT, 2016.

[28] PSA. PowerShift Atlantic Final Report, 2015.

[29] Ehsan Reihani, Mahdi Motalleb, Matsu Thornton, and Reza Ghorbani. A novel approach using flexible scheduling and aggregation to optimize demand response in the developing interactive grid market architecture. Applied Energy, 183:445–455, 2016.

[30] SEDC. Explicit demand response in Europe – mapping the markets 2017, 2017.

[31] F. Sirois, B. Bourdel, and R. P. Malhamé. Project RENE-034: Managing energy storage capacities dispersed in an electrical grid to reduce the effects of renewable energy source variability, 2017.

[32] J. Solis. Développement d'un estimateur d'état énergétique d'un chauffe-eau pour un contrôle par champ moyen. Master's thesis, Polytechnique Montréal, 2015.

[33] Adham I. Tammam, Miguel F. Anjos, and Michel Gendreau. Balancing supply and demand in the presence of renewable generation via demand response for electric water heaters. Annals of Operations Research, Online First, 2020.

[34] M. Wrinch, T. H. M. EL-Fouly, and S. Wong. Demand response implementation for remote communities. In 2011 IEEE Electrical Power and Energy Conference, pages 1–5, Oct 2011.

[35] Yue Zhou, Chengshan Wang, Jianzhong Wu, Jidong Wang, Meng Cheng, and Gen Li. Optimal scheduling of aggregated thermostatically controlled loads with renewable generation in the intraday electricity market. Applied Energy, 188:456–465, 2017.